JOURNAL OF VIROLOGY, Jan. 2006, p. 1015–1024 Vol. 80, No. 2
0022-538X/06/$08.00+0 doi:10.1128/JVI.80.2.1015–1024.2006

Low pH-Dependent Endosomal Processing of the Incoming Parvovirus Minute Virus of Mice Virion Leads to Externalization of the VP1 N-Terminal Sequence (N-VP1), N-VP2 Cleavage, and Uncoating of the Full-Length Genome

Bernhard Mani,[1] Claudia Baltzer,[1] Noelia Valle,[3] José M. Almendral,[3] Christoph Kempf,[1,2] and Carlos Ros[1,2]*

Department of Chemistry and Biochemistry, University of Bern, Freiestrasse 3, 3012 Bern,[1] and ZLB Behring AG, Wankdorfstrasse 10, 3000 Bern 22,[2] Switzerland, and Centro de Biología Molecular "Severo Ochoa," (Consejo Superior de Investigaciones Científicas-Universidad Autónoma de Madrid), 28049 Cantoblanco, Madrid, Spain[3]

Received 3 August 2005/Accepted 17 October 2005

Minute virus of mice (MVM) enters the host cell via receptor-mediated endocytosis. Although endosomal processing is required, its role remains uncertain. In particular, the effect of low endosomal pH on capsid configuration and nuclear delivery of the viral genome is unclear. We have followed the progression and structural transitions of DNA full-virus capsids (FC) and empty capsids (EC) containing the VP1 and VP2 structural proteins and of VP2-only virus-like particles (VLP) during the endosomal trafficking. Three capsid rearrangements were detected in FC: externalization of the VP1 N-terminal sequence (N-VP1), cleavage of the exposed VP2 N-terminal sequence (N-VP2), and uncoating of the full-length genome. All three capsid modifications occurred simultaneously, starting as early as 30 min after internalization, and all of them were blocked by raising the endosomal pH. In particles lacking viral single-stranded DNA (EC and VLP), the N-VP2 was not exposed and thus it was not cleaved. However, the EC did externalize N-VP1 with kinetics similar to those of FC. The bulk of all the incoming particles (FC, EC, and VLP) accumulated in lysosomes without signs of lysosomal membrane destabilization. Inside lysosomes, capsid degradation was not detected, although the uncoated DNA of FC was slowly degraded. Interestingly, at any time postinfection, the amount of structural proteins of the incoming virions accumulating in the nuclear fraction was negligible. These results indicate that during the early endosomal trafficking, the MVM particles are structurally modified by low-pH-dependent mechanisms. Regardless of the structural transitions and protein composition, the majority of the entering viral particles and genomes end in lysosomes, limiting the efficiency of MVM nuclear translocation.

Entry of viruses into host cells starts by binding to cell surface receptors, followed by penetration across the cellular membrane. Although cell entry of enveloped viruses is well characterized, the mechanisms of viral entry and nuclear targeting of nonenveloped viruses are still poorly understood. For many viruses, cell entry and uncoating are mediated by either receptor (pH independent), low pH, or both (19, 30, 31, 34, 39). The endocytic route has two main advantages for karyophilic viruses: one is the efficient and rapid transport toward the perinuclear area, and another is the exposure to a low pH, which can trigger conformational changes required for penetration, uncoating, and nuclear translocation.

In recent years, cell entry and nuclear targeting have gained great attention for parvoviruses, a group of small, nonenveloped viruses (8). *Minute virus of mice* (MVM) belongs to the *Parvovirus* genus. Its T=1 icosahedral capsid consists of two structural proteins, VP1 (82 kDa) and VP2 (63 kDa). A third protein, VP3, is produced after intracellular proteolytic cleavage, which removes approximately 25 amino acids from the N terminus of VP2 (47, 48, 53). VP1 and VP2 are identical in sequence except for the 143 amino acid residues at the N terminus of the VP1.

Although parvoviruses use different cellular receptors for attachment to the host cell, they are all internalized via receptor-mediated endocytosis and exposed to a low-pH environment. The endosomal acidification is known to be essential for the infection of parvoviruses (2, 3, 12, 16, 33, 36, 49); however, its specific role has not yet been elucidated. The site of endosomal release of the virus into the cytosol is also not well defined and may be influenced by the cell type. Adeno-associated viruses (AAVs) have been reported to escape from early endosomes and reach the nuclei within 40 min to 2 h (2, 54). Escape of AAV from late endocytic compartments has also been described (12, 16). AAV type 2 (AAV2) and AAV5 have also been detected in the trans-Golgi network (1, 32). Recently, it has been shown that the nuclear translocation of AAV particles was slower and more inefficient than previously described and that the majority of capsids accumulate in the perinuclear region (25). The endocytic traffic of canine parvovirus (CPV) and MVM seems to be slower than that of AAV. MVM requires reaching at least the late endosomal compartment, and replication in the nuclei was detected only after 8 h postinfection (p.i.) (36). CPV was found to accumulate in perinuclear vesicles resembling lysosomes (45), and like MVM, nuclear translocation was slow (52).

* Corresponding author. Mailing address: Department of Chemistry and Biochemistry, University of Bern, Freiestrasse 3, 3012 Bern, Switzerland. Phone: 41 31 6314349. Fax: 41 31 6314887. E-mail: carlos.ros@ibc.unibe.ch.

It is becoming increasingly evident that endosomal processing of incoming parvovirus particles is required and closely linked to the efficiency of nuclear translocation. When directly injected into the cytosol to circumvent the endocytic route, AAV2 failed to accumulate in the nuclei (10). CPV pretreated at low pH and injected into the cytosol was also unable to initiate progeny virus production (49). Despite these results, experimental data showing early conformational changes of parvovirus particles during the endocytic pathway are very limited.

With the exception of B19 (38), the unique N-terminal sequence (N-VP1) is internal in the parvovirus capsid and becomes exposed during the entry process (35, 46). N-VP1 can also be exposed by heat or urea (4, 7, 21, 50). The unique region of VP1 plays a central role in parvovirus biology. It harbors nuclear localization signals (NLSs) required for nuclear transport (51) that are essential for the incoming virion to initiate infection (22, 50) and the phospholipase A2 (PLA_2) motif, an activity that was not known to exist in viruses and that might be responsible for endosomal escape (5, 11, 15, 56). Although N-VP1 externalization outside the viral coat is required prior to nuclear penetration of the genome, a role of endosomal acidification in this externalization process has not been found. Treatment of cells with lysosomotropic drugs did not prevent the externalization of CPV N-VP1, and heat-induced exposure of N-VP1 prior to virus inoculation did not improve the infection in the presence of acidification-blocking drugs, suggesting that there might be some other low-pH-dependent factors which are required for the infection (46).

Another capsid modification that has been observed during the entry process of CPV and MVM is the cleavage of N-VP2 to form VP3 (47, 48, 53). The N-VP2 has been found to function as a nuclear export signal for the maturing virions with encapsidated genome (28). However, so far, the intracellular site, the mechanism, and the role of the VP2 cleavage during the entry process have not been elucidated.

The purpose of the present study was to examine the capsid structural rearrangements occurring during the endosomal processing of MVM. Several minutes after infection, when the virus was located within endosomal vesicles, three major capsid rearrangements were already evident: N-VP1 externalization, N-VP2 cleavage, and the exposure of the full-length genome. In addition to their simultaneous appearance, all three changes were similarly impaired by raising the endosomal pH. Interestingly, regardless of these structural changes, the bulk of the incoming MVM capsid was retained within lysosomes. Thus, the inefficient escape from the endosomal compartment represents the major barrier for the cellular invasion of the incoming MVM virion.

MATERIALS AND METHODS

Cells and viruses. Mouse A9 fibroblasts were propagated in Dulbecco's modified Eagle's medium (DMEM) supplemented with 10% heat-inactivated fetal calf serum. Stocks of MVM without detectable levels of VP3 were prepared by infection of A9 cells. When the cytopathic effect was becoming evident, the supernatant was collected and cleared by low-speed centrifugation, thus discarding the intracellular virions rich in VP3. Titers were determined by quantitative PCR as DNA-containing particles per microliter. Gradient-purified MVM full-virus (FC) and empty (EC) capsids were prepared as previously described (22). VP2-only virus-like particles (VLP) were produced and purified from Sf9 insect cells with a baculovirus system, as previously described (18).

Radiolabeling and purification of MVM particles. The method employed was basically as previously described (27). In brief, cells were infected with MVM and labeled from 4 to 48 h postinfection in methionine-free DMEM supplemented with 200 μCi/ml of [^{35}S]methionine (Amersham Biosciences, Buckinghamshire, United Kingdom). At the end of the labeling periods, cells were harvested into the medium supplemented with protease inhibitors and 0.2% sodium dodecyl sulfate (SDS). Cell debris was removed by low-speed centrifugation, and homogenates were centrifuged for 5 h and 30 min at 217,000 × *g* through 2 volumes of a 20% sucrose cushion. The resuspended pellets were adjusted to a density of 1.38 g/ml in CsCl by refractometry and centrifuged to equilibrium for 24 h at 170,000 × *g*. The label distribution was determined by scintillation counting, and fractions containing labeled particles with a density corresponding to empty MVM capsids (1.32 g/ml) and DNA full virions (1.39 to 1.41 g/ml) were pooled and extensively dialyzed against phosphate-buffered saline.

Antibodies. Rabbit anti-VPs (polyclonal against MVM structural proteins), rabbit anti-N-VP2 (polyclonal against the N terminus of VP2), and mouse anti-capsid (monoclonal against intact capsids; clone B7) antibodies have been described elsewhere (23, 24, 28). A rabbit polyclonal antibody against the N terminus of VP1 was kindly provided by P. Tattersall (7). Rabbit anti-actin antibody (sc-10731), goat anti-mouse fluorescein isothiocyanate (FITC) (sc-2010), goat anti-mouse rhodamine (sc-2092), goat anti-rabbit FITC (sc-2012), and goat anti-rabbit rhodamine (sc-2091) were purchased from Santa Cruz Biotechnology (Santa Cruz, Calif.). Goat anti-rabbit horseradish peroxidase-conjugated antibody was purchased from DakoCytomation (Glostrup, Denmark).

Chemicals. Aclarubicin, bafilomycin A_1 (BA), brefeldin A (BFA), chloroquine (CHLO), pepstatin A, *N*-tosyl-L-phenylalanine chloromethyl ketone (TPCK), and *N*α-*p*-tosyl-L-lysine chloromethyl ketone (TLCK) were purchased from Sigma (St. Louis, Mo.). Aprotinin, E64, and MG132 were obtained from Calbiochem (La Jolla, Calif.). Dimethyl sulfoxide was used to dissolve MG132, pepstatin A, and TPCK. Aprotinin, chloroquine, E64, and TLCK were dissolved in water, and aclarubicin, BA, and BFA in ethanol. All drugs were stored at −20°C. Lysine-fixable dextran Texas Red (10 kDa) (Molecular Probes, Eugene, Ore.) was dissolved in DMEM and stored at 4°C.

Immunofluorescence. A9 cells (10^5) were seeded onto coverslips within 12-well plates. After 24 h, the cells were infected with 10,000 DNA-containing particles, per cell, corresponding to approximately 1 PFU/cell (40), for 1 h at 4°C, subsequently washed to remove unbound virus, and incubated at 37°C. At different times, cells were washed and processed for immunofluorescence as previously described (22, 23) with secondary antibodies coupled to rhodamine or FITC. Cells were mounted with Mowiol (Calbiochem) containing 30 mg/ml of DABCO (Sigma) as an antifading agent and examined by fluorescence microscopy, and images were captured with the proper filter sets and a 100× oil immersion objective.

Examination of VP2 cleavage. A9 cells (10^5) were infected with MVM stocks (1 PFU/cell) without detectable levels of VP3, as indicated above. At different intervals, as specified in Fig. 1, cells were lysed in protein loading buffer and resolved by SDS–10% polyacrylamide gel electrophoresis (PAGE). After transfer to a polyvinylidene difluoride membrane, the blot was probed with a rabbit anti-VP antibody (1:2,000 dilution), followed by a horseradish peroxidase-conjugated secondary antibody (1:20,000 dilution). The viral structural proteins were visualized with a chemiluminescence system (Pierce, Rockford, IL). Additionally, the intracellular cleavage of VP2 was also examined in purified full-virus and empty capsids and by immunofluorescence.

The effect on the cleavage of endosome- and proteosome-blocking agents as well as protease inhibitors was examined. A9 cells were infected as specified above in the presence of one of the following drugs: BA (150 nM), CHLO (100 μM), BFA (5 μg/ml), MG132 (25 μM), aclarubicin (0.1 μM), TPCK (20 μM), TLCK (20 μM), aprotinin (2 μg/ml), E64 (10 μM), and pepstatin A (1 μM). At 0, 2, and 24 h p.i., cells were lysed in protein loading buffer and viral proteins detected as specified above.

In situ hybridization. Biotinylated probes specific for the 3′ and 5′ regions of the MVM genome, as well as for the 3′ region of human parvovirus B19 (used as a negative control), were generated from PCR products by nick translation (Roche Diagnostics, Mannheim, Germany) according to the manufacturer's instructions. The PCR products for the biotinylation were obtained with the following primers: the MVM 3′ region (5′-GACGCACAGAAAGAGAGTAACC AA-3′ from nucleotides 230 to 254 and 5′-TGCTGGCTGGTCCATGAAAT-3′ from nucleotides 1447 to 1467), the MVM 5′ region (5′-CGCTACACATGGG ATGAAACAA-3′ from nucleotides 3975 to 3997 and 5′-CAGTTGGTTCACT GAATAGACAGTAGT-3′ from nucleotides 4912 to 4939), and the B19 3′ region (5′-CCTGGACTTTCTTGCTGTT-3′ from nucleotides 548 to 566 and 5′-GCCCATAAAACCACAGTGTA-3′ from nucleotides 1581 to 1600). The

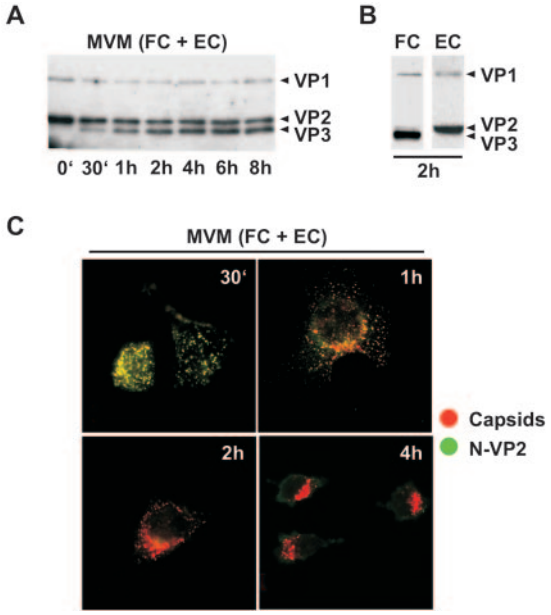

FIG. 1. Kinetics of N-VP2 cleavage. (A) A9 cells (10^5) were infected with nonpurified MVM stocks (one PFU per cell) without detectable levels of VP3. At different intervals postinfection, the viral structural proteins were analyzed by 10% PAGE. After transfer to a polyvinylidene difluoride membrane, the blot was probed with a rabbit anti-VP antibody, followed by a horseradish peroxidase-conjugated secondary antibody. (B) Western blot analysis of purified FC and EC at 2 h postinfection. (C) A9 cells were infected with MVM stocks as indicated above. At different intervals postinfection, the cleavage of VP2 was examined by immunofluorescence with an antibody against capsids (red) and antibody against the N-VP2 (green).

sizes of the hybridization probes were 200 to 500 nucleotides in length, as confirmed by agarose gel electrophoresis.

Infected cells were fixed and immunostained with the monoclonal antibody (MAb) B7 and incubated in a humid chamber at 37°C for 18 h with a volume of 20 μl hybridization mix (5 ng/μl biotinylated probe in 60% deionized formamide, 300 mM NaCl, 20 mM sodium citrate, 10 mM EDTA, 25 mM NaH_2PO_4 [pH 7.4], 5% dextran sulfate, 250 ng/μl sheared salmon sperm DNA). Subsequently, the slides were washed (50% deionized formamide, 25 mM NaCl, 2.5 mM sodium citrate [pH 7.4]) three times for 5 min at room temperature and once at 37°C. The samples were blocked for 30 min with 1% blocking solution (Roche) in 150 mM NaCl–100 mM Tris-HCl, pH 7.4. Biotin was detected with avidin-rhodamine (Roche) at 1:500 in blocking solution for 45 min. Finally, the cells were washed three times for 10 min (200 mM Tris-HCl [pH 7.4], 1.5 M NaCl, 0.05% Tween 20), mounted with Mowiol, and examined by fluorescence microscopy.

Cytoplasmic and nuclear distribution of radiolabeled virus particles. A9 cells (10^5) were infected with radiolabeled full-virus capsids (1 PFU/cell). After 1 h (background control for viral nuclear accumulation) and 18 h, nuclei and cytoplasm were separated by using the Nuclear/Cytosol fractionation kit from BioVision (Mountain View, Calif.) according to the manufacturer's instructions. The purity of the fractions was verified by the detection of β-actin protein as a cytoplasmic marker. Nuclear integrity was examined with a hemocytometer chamber. The proteins present in the nuclear and cytoplasmic fractions (nucleus/cytoplasm ratio, 1:1) were separated by SDS-PAGE. The gel was fixed in isopropanol-water-acetic acid (25:65:10) for 30 min, soaked with Amplify fluorographic reagent (Amersham) for 30 min, dried under a vacuum, and exposed to an autoradiography film.

The infectivity of the radiolabeled full-virus capsids was determined in parallel analyses by scraping the A9 cells at, 8, 18, and 24 h p.i. The total DNA was extracted from the cell pellet by using the DNeasy tissue kit (QIAGEN, Valencia, Calif.), and virus DNA was quantified by real-time PCR, as specified below.

Real-time PCR. Quantitative PCR was used to detect and quantify viral DNA. Primers for MVM DNA amplification were as follows: forward (5′-GACGCAC AGAAAGAGAGTAACCAA-3′ from nucleotides 231 to 254) and reverse (5′-CCAACCATCTGCTCCAGTAAACAT-3′ from nucleotides 709 to 732). Amplification and real-time detection of PCR products was performed by using the FastStart DNA SYBR Green kit (Roche) following the manufacturer's instructions. As external standards, the PCR products generated by the above primers were cloned into the pGEM-T vector (Promega, Madison, Wis.) and used in 10-fold dilutions.

Evaluation of the lysosomal membrane integrity. The integrity of the lysosomal membranes of A9 cells inoculated with FC, EC, and VLP was examined with the fluid-phase late endocytic marker dextran Texas Red (Molecular Probes). A9 cells (10^5) grown on coverslips were infected with 1 PFU/cell of FC or with comparable amounts (as assessed by Western blotting) of EC and VLP for 1 h at 4°C. Subsequently, the cells were washed to remove unbound viral particles and incubated at 37°C in the presence of dextrans of 10 kDa (dissolved in DMEM to a concentration of 2.5 mg/ml). After 15 min, the cells were intensively washed with phosphate-buffered saline and further incubated at 37°C. After various times postinfection, the cells were fixed and the viral intact capsids were immunostained with MAb B7 as specified above.

RESULTS

Kinetics of the intracellular cleavage of VP2. A variable but high proportion of the N termini of the capsid protein VP2 of full MVM particles is exposed on the surface, but it is sequestered in empty MVM capsids (7). VP3 is generated by the proteolytic cleavage of approximately 25 amino acids of the VP2 N terminus of DNA full-virus capsids (6, 47). The kinetics of the cleavage was investigated using Western blot analysis and immunofluorescence microscopy with an antibody raised against the N terminus of VP2 (27). Binding of the virus with its receptor did not trigger the cleavage, which started only a few minutes after internalization and was complete by 2 h (Fig. 1A). Since this experiment was performed with a nonpurified MVM preparation, which contains similar amounts of both full-virus and empty capsids, the cleavage occurred in only half of the particles. Correspondingly, Western blot analysis of purified FC and EC at 2 h postinfection showed that only FC are cleaved (Fig. 1B). The same cleavage kinetics were observed by immunofluorescence using antibodies against intact virus capsids (MAb B7) and against the N terminus of VP2. Both antibodies colocalized during the first minutes postinfection. However, the signal from the N-VP2 antibody progressively decreased with the increasing postinternalization times and by 2 h, was no longer detected (Fig. 1C). Since the occurrence of the cleavage coincides with the early endosomal trafficking of MVM, these results demonstrated that the cleavage of VP2 to VP3 is performed within the endosomal vesicles. The fact that the N-VP2 of EC is detected by Western blotting (Fig. 1A and 1B) but not by immunofluorescence (Fig. 1C, from 2 h p.i.) indicated that it remains inside the capsid during the intracellular trafficking. Similar to EC, the N-VP2 of VLP was not cleaved or detected by immunofluorescence, suggesting that it also remained in the interior of the capsid (data not shown).

Endosomal exposure of the N-VP1 sequence in FC and EC particles. The N-terminal sequence of the capsid protein VP1 harbors the NLS and PLA_2 motifs, which were shown to be essential for virus infection (5, 11, 15, 22, 50, 56). The N-VP1 of MVM is initially buried inside the virion (7), and thus, it should be externalized outside the coat to mediate both phospholipase and nuclear targeting functions. The N-VP1 externalization kinetics was examined by immunofluorescence in order to define the timing and the cellular compartment where it occurs. Following receptor binding and 10 min postinternalization, the N-VP1 of FC was still buried inside the virion.

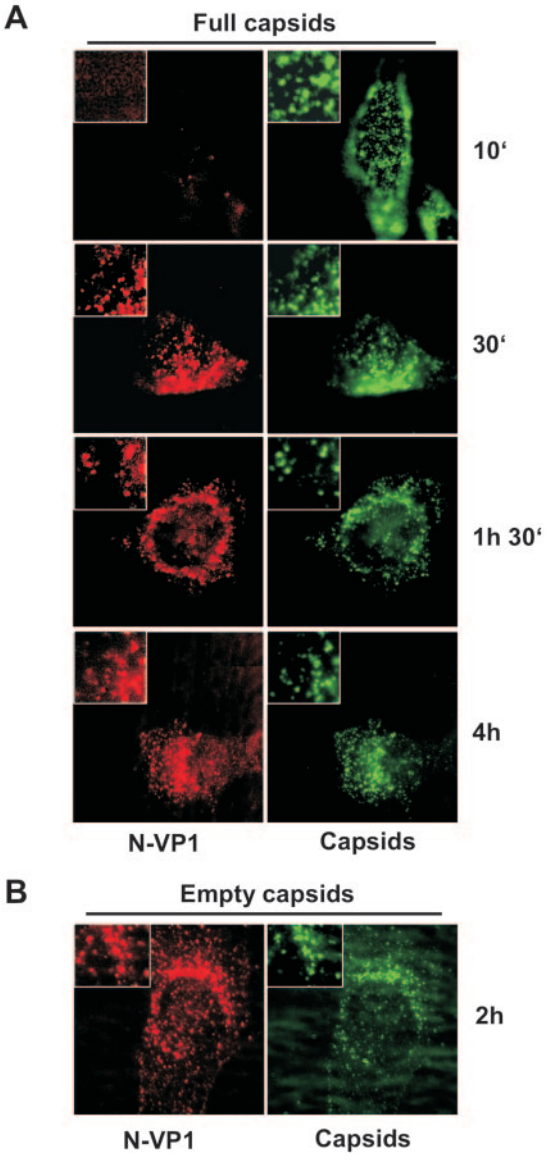

FIG. 2. Kinetics of N-VP1 externalization. (A) Externalization of N-VP1 from full-virus capsids was examined by immunofluorescence at various times postinfection. Antibody against capsids (green) and antibody against the N-VP1 (red) are shown. (B) Externalization of N-VP1 from empty capsids was examined at 2 h postinfection.

However, as early as 30 min postinternalization, it became exposed and colocalized with intact virus capsids (Fig. 2A). This observation confirmed that the externalization occurs in early endocytic vesicles. Similar to full-virus capsids, EC also exposed the N-VP1 (Fig. 2B) and with similar kinetics (data not shown), while N-VP1 was not detected in cells inoculated with VLP (data not shown). This observation indicates that, at least for EC, neither the viral DNA nor the cleavage of N-VP2 has influence on N-VP1 externalization in intact particles.

Early endosomal processing of MVM capsids leads to the externalization of full-length viral DNA. For many viruses, the process of uncoating commences early after infection triggered by cellular factors, including receptor binding and low endosomal pH (44). We have examined by in situ hybridization whether the single-stranded DNA (ssDNA) of MVM becomes accessible during the endosomal progression of the virus. MVM-specific probes covering the 3′ and 5′ regions of the viral genome were applied (Fig. 3A). After receptor binding and the first minutes postinfection, the viral DNA was still packed inside the FC and not accessible to the probes. However, and coinciding in postinfection time with the N-VP2 cleavage and the N-VP1 externalization, the genome of the incoming particles became exposed in its full length (Fig. 3B). The signals generated by the 3′ and 5′ probes were similar in intensity and kinetics. Up to 8 h p.i., the signal colocalized with assembled viral capsids (MAb B7) in the cytoplasm. However, at 21 h p.i., when the replication plateau has been achieved, the incoming particles were still detected in the perinuclear lysosomal vesicles, but the viral DNA was detected exclusively in the nuclei, corresponding to de novo virus DNA synthesis. No signal was detected in cells when using a probe derived from parvovirus B19 sequences or when inoculating cells with MVM empty capsids (Fig. 3C).

The loss of perinuclear viral DNA signal was further investigated in infected nonproliferating cells. As shown in Fig. 3D, the perinuclear viral DNA signal could be stabilized by cell starvation. This result may suggest that DNase II, a lysosomal enzyme whose activity peaks during the S phase and is low in quiescent cells (43), could be involved in the degradation of the exposed viral DNA within lysosomal vesicles.

VP2 cleavage, N-VP1 externalization, and uncoating can be blocked by raising the endosomal pH. The three capsid structural rearrangements, N-VP2 cleavage, N-VP1 externalization, and viral DNA uncoating, start within the first minutes postinfection. At this time, MVM is located within the acidified endosomal vesicles (36). Since the endosomal acidification is required for MVM infection (36), it was therefore of interest to investigate whether the low endosomal pH is involved in the viral capsid rearrangements. Infection of A9 cells with MVM was carried out in the presence or absence of chloroquine, a drug that raises the endosomal pH, and the structural modifications of the capsids were examined by 6 h p.i. While in control untreated cells, the capsid modifications had been accomplished, none of which were detected in treated cells (Fig. 4).

The effect of drugs that block different intracellular pathways on the VP2 cleavage was further examined. As shown in Fig. 5A, only drugs disturbing the endosomal pH had an effect. Brefeldin A, a drug that blocks the early-to-late endosome transitions, had no effect, suggesting that the VP2 cleavage must be performed in early endosomes. This result is in agreement with the fast kinetics of the cleavage (Fig. 1). Additionally, the protease involved in the cleavage was investigated. Infection of A9 cells with MVM in the presence of different protease inhibitors showed that only the chymotryptic inhibitor TPCK was able to disturb the cleavage (Fig. 5B) and block the infection. However, it should be mentioned that TPCK also blocks the chymotryptic activity of the proteasome, which has been previously shown to be required for MVM infection (36). Furthermore, as demonstrated in reference 35 and shown in Fig. 5A, the proteasome is not involved in the cleavage of VP2, as other drugs blocking the proteasome do not block the cleavage. However, the TPCK block of the MVM infection may occur at several levels, for example, as an inhibition of the

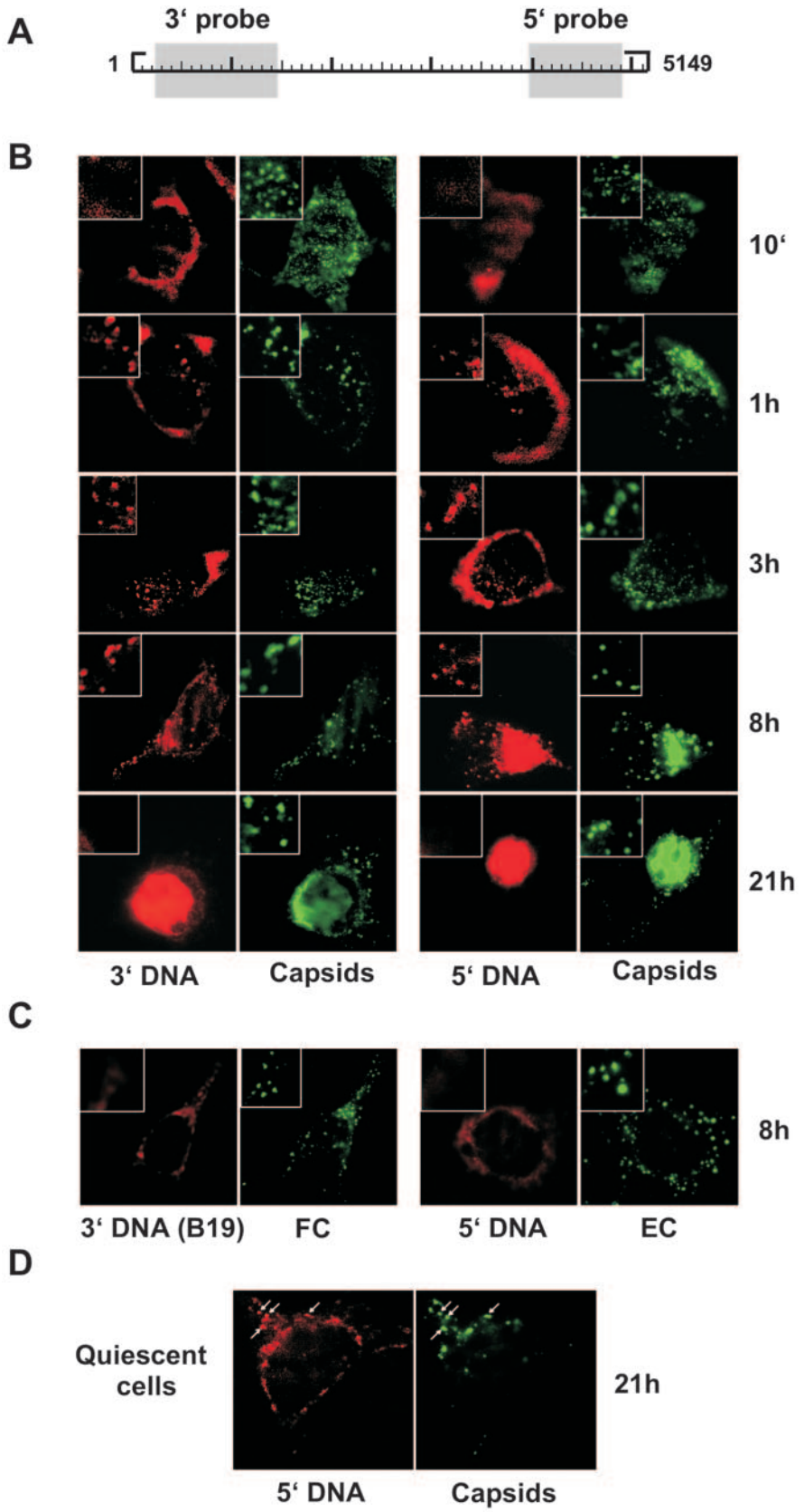

FIG. 3. Detection of full-length genome externalization during the endosomal trafficking of MVM. (A) MVM genomic regions covered by the probes are shadowed. (B) A9 cells (10^5) seeded onto coverslips were infected with MVM as specified in Materials and Methods. At various times postinfection, the presence of externalized viral DNA was examined by in situ hybridization with probes covering the 3′ or 5′ regions of the MVM genome (red) and the viral capsids were detected with the MAb B7 against assembled virions (green). (C) Negative controls: cells infected with FC and hybridization with an unrelated MVM probe (derived from B19 sequences). Cells inoculated with empty particles and hybridization with the 5′ MVM probe. (D) Detection of exposed viral DNA at 21 h postinfection in quiescent cells.

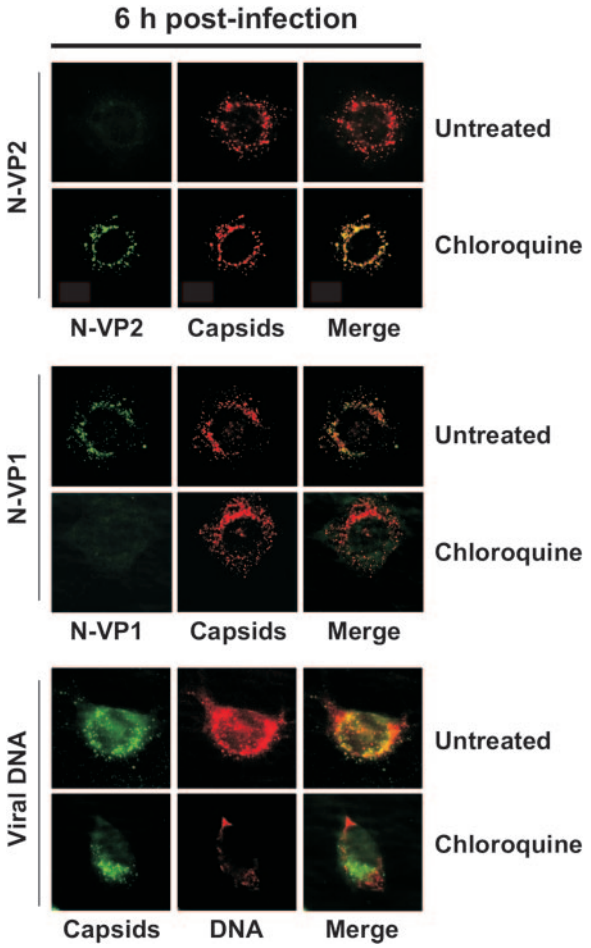

FIG. 4. Effect of chloroquine on the N-VP2 cleavage, N-VP1 externalization and uncoating. A9 cells (10^5) were infected with MVM. At 6 h postinfection, the presence of N-VP2, N-VP1, and the 5′ region of the viral genome was examined by immunofluorescence in the presence or absence of chloroquine (100 μM). The virus capsids were detected with the MAb B7 (against assembled capsids).

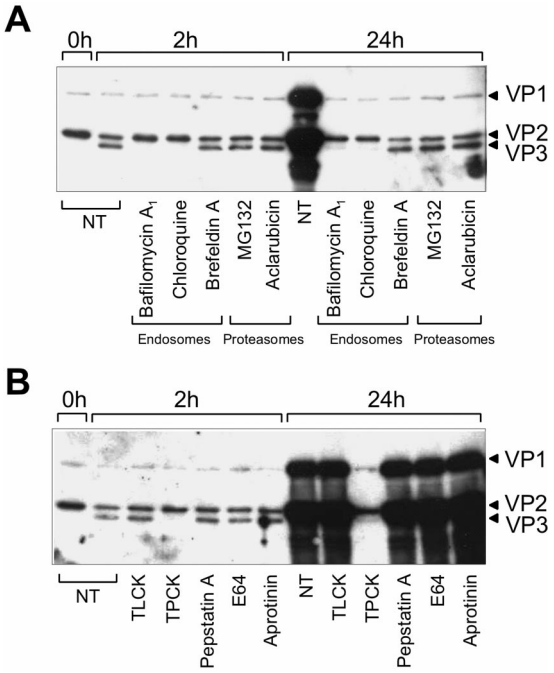

FIG. 5. Blocking of VP2 cleavage in vivo. (A) Effect of endosome- and proteasome-disturbing agents on VP2 cleavage. A9 cells were infected with MVM stocks without VP3 in the presence of one of the following inhibitors: BA (150 nM), CHLO (100 μM), BFA (5 μg/ml), MG132 (25 μM), or aclarubicin (0.1 μM). (B) Effect of protease inhibitors on the VP2 cleavage. A9 cells were infected in the presence of one of the following inhibitors: TPCK (20 μM), TLCK (20 μM), aprotinin (2 μg/ml), E64 (10 μM), or pepstatin A (1 μM). At 0, 2, and 24 h postinternalization, cells were lysed in protein loading buffer and viral proteins were detected. NT, nontreated.

proteasome unrelated to the VP2 cleavage or of the cleavage itself prior proteasome requirement.

The bulk of incoming FC, EC, and VLP are retained within the lysosomal compartment without signs of lysosomal membrane destabilization. The accumulation of FC, EC, and VLP in the lysosomal compartment was confirmed by the colocalization of incoming particles with coendocytosed dextrans (Fig. 6A). At 18 h p.i., when the replication plateau was achieved, the majority of viral FC still colocalized with dextrans of 10 kDa (Fig. 6A). Since EC and VLP cannot produce progeny virions, we could study their endosomal trafficking for longer periods of time after internalization. At up to 50 h p.i., both EC and VLP could still be detected as intact (MAb B7 staining) and colocalizing with dextrans. The bulk of the FC remained intact inside the lysosomal compartment having had both N-VP1 externalized and N-VP2 cleaved (Fig. 6B). Despite the external disposition of the N-VP1 (with its PLA_2 motif), the coendocytosed dextrans of 10 kDa were not released and remained inside the lysosomal vesicles colocalizing with the assembled virions (Fig. 6A). These results indicated that the endosomal escape is the major limiting factor for the subsequent MVM intracellular traffic.

Nuclear targeting by MVM is very inefficient. Parvovirus replication takes place in the nuclei, but the nature of the infectious entity penetrating into the nuclei remains unknown. The NLS motif present in the N-VP1 is essential for CPV infection (50) as well as for the entering MVM virion to initiate infection (22). These data imply that the parvoviral genome must be translocated into the nucleus or docked to the nuclear pore in association with at least some VP1 subunits, and some experimental data may suggest that this association involves the capsid itself (2, 41, 42, 54). In order to address whether the viral DNA enters the nuclei naked or associated with viral proteins, the accumulation of incoming FC proteins in the nuclei was examined. A9 cells were infected with radiolabeled MVM virions, and the presence of radiolabeled viral proteins in the nuclear and cytoplasmic fractions was determined at 1 h p.i. (background control for the nuclear viral proteins) and 18 h p.i., when the replication plateau was achieved (Fig. 7B). As shown in Fig. 7A, there was no detectable increase of viral proteins over the background level (1 h p.i.) in the nuclear fraction at 18 h p.i., as well as no decrease in the level of viral proteins accumulated in the cytoplasmic fraction. This result implies that the infectious entity penetrating into the nuclei consists of free viral DNA devoid of structural proteins or of a very limited level of a viral nucleoprotein complex.

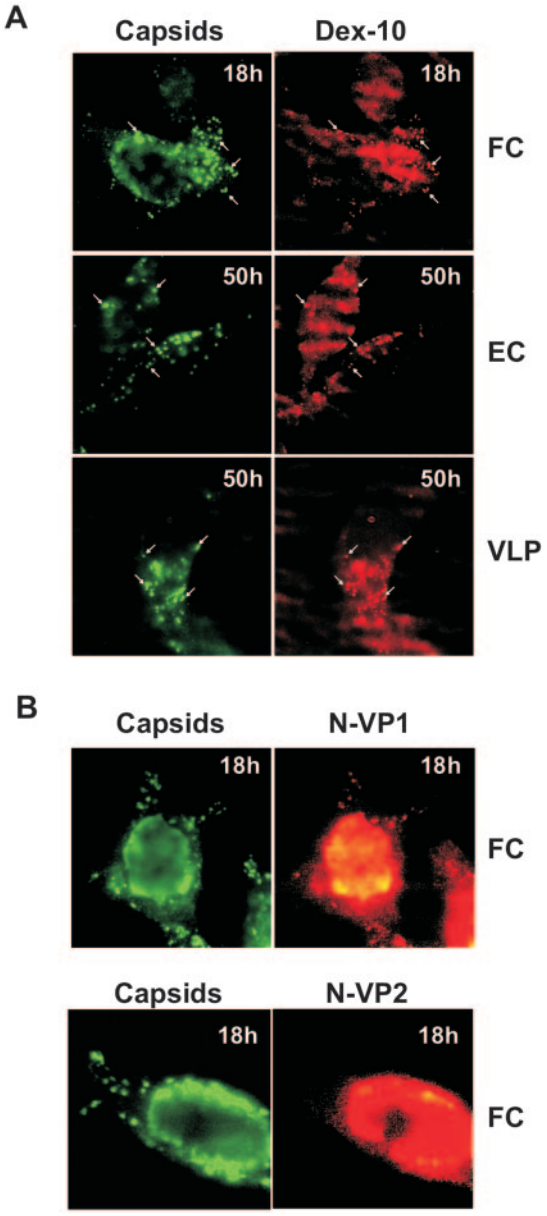

FIG. 6. Effect of incoming full-virus, empty capsids, and virus-like particles on lysosomal membrane integrity. (A) The integrity of the lysosomal membranes from A9 cells infected with full-virus capsids, empty capsids, or VLP was examined with the 10-kDa fluid-phase lysosomal marker dextran Texas Red (Dex-10; red). The integrity of the viral capsids was examined with the MAb B7 against assembled capsids (green). (B) Externalization of N-VP1 and cleavage of N-VP2 examined at 18 h p.i. in cells infected with FC.

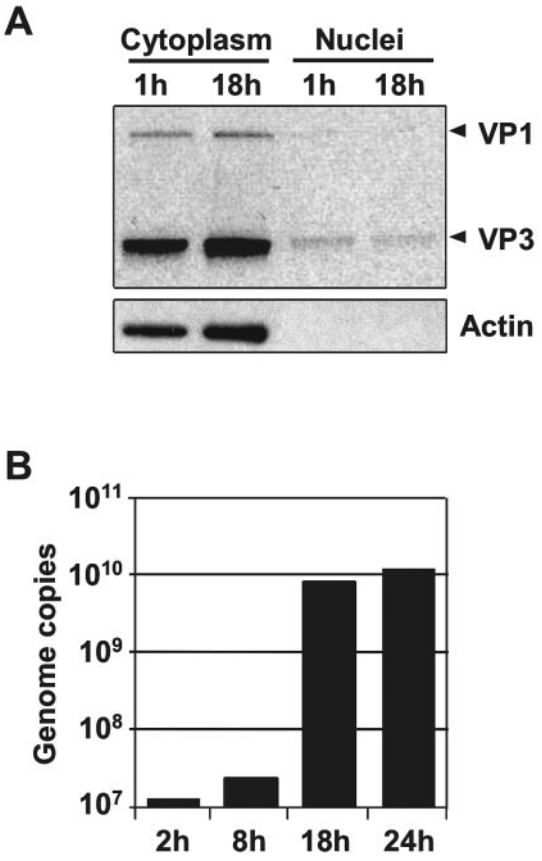

FIG. 7. Cytoplasmic and nuclear distribution of radiolabeled viral proteins. (A) A9 cells were infected with radiolabeled full-virus capsids (1 PFU per cell). After 1 h (background control for viral nuclear accumulation) and 18 h p.i., nuclei and cytoplasm were separated and the viral proteins present in the nuclear and cytoplasmic fractions (nuclei/cytoplasm ratio, 1:1) were examined. (B) DNA replication kinetics of the radiolabeled full-virus capsids. A9 cells were infected (1 PFU per cell). After 2, 8, 18, and 24 h p.i., the viral DNA was quantified by real-time PCR.

DISCUSSION

Parvoviruses enter the host cell via receptor-mediated endocytosis, though the endosomal trafficking seems to vary slightly depending on the parvovirus and host cell. A common aspect is that the endosomal processing of the incoming viral particles is crucial for the infection, influencing the efficiency of the nuclear translocation. When parvovirus particles are injected directly into the cytosol to circumvent the endocytic route, they fail to accumulate in the nuclei (10, 49). Despite the evidence that native parvovirus particles require a maturation step through the endosomal pathway, experimental data showing conformational changes of the particles during the endocytic route are very limited. In the present study, we aimed at identifying the structural changes associated with traffic through the endosomal network of MVM. Three different viral particles were used: FC, containing the viral DNA; EC, devoid of DNA; and VLP, devoid of both VP1 and DNA. These three types of viral particles bind and compete for the same primary receptor in MVM-permissive A9 mouse fibroblasts (40).

Conformational transitions of MVM capsids along endosomal trafficking. Originally inside the capsid (except for B19) (38), the unique N-VP1 of parvovirus becomes exposed in vivo during the entry process (35, 50) or in vitro by heat or urea (4, 7, 21, 50). Although it has not been directly shown to occur within the endosomal compartments, the externalization of N-VP1 from CPV occurs in the cytoplasm as early as 2 h postinfection (46). Different from MVM, treatment of cells with bafilomycin, which raises the endosomal pH, did not prevent the externalization of CPV N-VP1, and heat-induced ex-

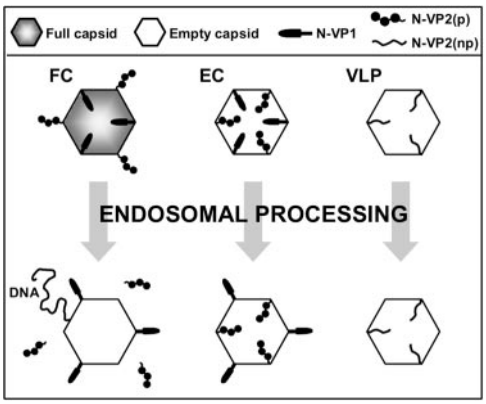

FIG. 8. Schematic representation of the capsid rearrangements during the endosomal trafficking of MVM virions (FC), EC, and VLP. The amounts and ratio of the represented viral proteins do not correspond to the amounts and ratio in the natural capsid. p, phosphorylated; np, nonphosphorylated. The symbols are the same as those used in reference 28.

ternalization of N-VP1 prior to infection did not improve the infection in the presence of acidification-blocking drugs, suggesting that there might be some yet-unidentified low-pH-dependent factors, which are required for the infection (46).

Thirty minutes after internalization, FC and EC externalized the N terminus of VP1, which remained stable and colocalizing with intact particles in the cytoplasm for long periods of time (Fig. 2 and 6B). The fact that EC were able to expose the N-VP1 indicates that encapsidation of the viral DNA, which determines the externalization of an important proportion of the N-VP2 during virus maturation in the nuclei (7), does not play a role in the extrusion of the N-VP1 at the low endosomal pH. Noteworthy previous studies have shown that a significant proportion of the N-VP2 from EC and VLP can be externalized by moderate heating and be cleaved by trypsin digestion (18), but N-VP1 is apparently not exposed in EC or is resistant to cleavage (see below). However, in the intracellular traffic, the EC and VLP did not expose N-VP2, whereas EC did expose N-VP1 sequences (Fig. 1 and 2). These results indicate that the heat treatment in vitro may not strictly reproduce the low-pH-induced structural changes of the MVM capsid occurring in vivo.

Two other additional capsid rearrangements were observed in only FC, namely, the externalization of the full-length viral genome and the cleavage of the N terminus of VP2. It is intriguing that N-VP1 is exposed in FC and EC in the same endosomal compartment as the N-VP2 in FC; however, it is not cleaved. A possible explanation for the lack of intracellular N-VP1 cleavage and by trypsin in vitro in heated EC (18) may be the different pattern of phosphorylation between both polypeptides assembled in MVM capsids (27), which may rend the cleavage sites within the VP1-specific sequence refractory to proteases. An alternative explanation could also be that the externalized N-VP1 recognized by the polyclonal antibody represents only a short amino acid sequence of the N terminus, not including accessible trypsin cleavage sites.

The capsid structural rearrangements observed in this work for the three types of MVM particles along the endosomal trafficking are summarized in Fig. 8. All three structural changes occurred simultaneously within the first hour postinternalization, and all of them were similarly impaired by drugs raising the endosomal pH, confirming their occurrence within the endosome through a low-pH-dependent mechanism. The simultaneous externalization of N-VP1 and the viral DNA from intact capsids have been previously shown to occur in vitro (4, 7), suggesting that the conformational change leading to N-VP1 externalization would also lead to DNA externalization. Sustaining this notion is our observation in vivo that N-VP1 and the viral DNA are externalized simultaneously and both depend on the low pH (Fig. 2 to 4). In vitro studies showed that upon brief heating of the capsid of MVM, the viral DNA is externalized in its full length without capsid disassembly and that the externalization is facilitated in parvovirus B19 capsids, which have N-VP1 already exposed (37). Finally, the endosomal progression of VLP was similar to that of FC and EC, indicating that VP1 and the viral DNA have no influence on the traffic of the capsid through the endosomal network.

MVM capsid stability and lysosomal accumulation. The observed conformational transitions do not affect the capsid integrity, which remains essentially intact. The incoming capsids were followed by immunofluorescence with the MAb B7, previously described to react against a conformational epitope on the MVM capsid (23, 24). As shown in Fig. 6, antibody B7 reacted with cytoplasmic FC at 18 h p.i. The detected cytoplasmic full-virus capsids are the incoming and not de novo particles, since they colocalized with dextrans of 10 kDa, a lysosomal marker. Given that EC and VLP are not infectious, we could follow their capsid integrity and intracellular progression for longer periods of time. As shown in Fig. 6, EC and VLP were still intact at least up to 50 h p.i. and colocalizing with the lysosomal marker.

The accumulation and persistence of the incoming particles within lysosomes did not result in the degradation of the highly resistant capsid. However, the exposed viral DNA of FC was no longer detected in lysosomes (Fig. 3B, 21 h p.i.). Apart from the site of intracellular and extracellular protein degradation (9, 13, 29), the lysosome also degrades foreign DNA through the activity of the lysosomal endonuclease DNase II (14). Accordingly, the loss of the cytoplasmic DNA signal was most probably due to the degradation of the exposed unprotected ssDNA by the ubiquitous lysosomal enzyme DNase II. The optimal pH of DNase II is 5.0; however, its activity can be detected over a significant pH range (26). DNase II is active mainly against double-stranded DNA, although less effectively, it also degrades ssDNA (55). It has been previously observed that a significant amount of incoming AAV ssDNA is degraded during the first 48 h postinfection. This degradation was attributed to the activity of intracellular nucleases (17). In relation to the cell cycle, DNase II is most active during the S phase and its activity drops in quiescent cells (43). Interestingly, reduction of the lysosomal DNase II activity by cell starvation also reduced the degradation of the viral DNA (Fig. 3D). This result supports the notion that a large proportion of the incoming MVM genomes are degraded inside the lysosomes.

The persistence of MVM particles within lysosomes seems to be due to the inability of the virions to permeabilize the lysosomal membrane by the PLA_2 activity of the exposed N-VP1. As shown in Fig. 6A, FC, EC, and VLP were unable to release coendocytosed dextrans of 10 kDa. Similar results were

obtained in cells infected with CPV (46). It has been previously shown in vitro that the activity of parvovirus PLA_2 is optimal at pH 6 to 7 and decreases at pH 5 (5). Accordingly, the highly acidic environment of the lysosomes would not represent the best conditions for the function of PLA_2. All these observations open two main interpretations. One is that only a minor subset of lysosomes is disrupted/permeabilized by the PLA_2 activity of the incoming MVM; the other is that few viruses escape from a prelysosomal vesicle without membrane disruption. Supporting the latter hypothesis is the fact that the N-VP1 externalization, which is required for endosomal escape, occurs only a few minutes after internalization. Therefore, the viral PLA_2 is set before the incoming virions reach the lysosomes. Considering that blocking the transition between early and late endosomes also blocks the infection (36), it is likely that few incoming virions enter the cytosol through an intermediate prelysosomal vesicle, notably, late endosomes.

Endosomal escape as the major limiting factor of MVM nuclear translocation. The amount of virus particles able to penetrate into the cytosol seems very restricted, as shown by the massive accumulation and retention of the incoming particles in the lysosomal compartment. In agreement with the inefficient endosomal escape, the infection of cells with radiolabeled full-virus capsids showed no detectable accumulation of incoming viral proteins in the nuclei, and the amount of cytoplasmic virus remained unchanged before and after the viral replication reached a plateau (Fig. 7). The results obtained with EC and VLP are particularly interesting. EC are structurally similar to FC, and N-VP1 (with its PLA_2 motif) is similarly exposed on the capsid surface (Fig. 2B). VLP do not contain VP1; thus, without PLA_2, they should not be able to escape from endosomes. EC and VLP are not infectious (empty particles), and therefore, their cytoplasmic trafficking can be studied for long periods of time without the interference of the viral progeny. Despite the fact that EC have N-VP1 and that it becomes exposed, both EC and VLP accumulated similarly in lysosomes for very long periods of time after infection and were similarly unable to release dextrans of 10 kDa (Fig. 6A). These results suggest that only a few undetectable incoming viral proteins penetrate into the nuclei. One other possibility is that following the uncoating of the virus in the cytoplasm, which was actually observed in the present study, and the transport of the resulting nucleoprotein complex to the nuclear pore, the viral DNA translocates into the nuclei devoid of structural proteins. Independent of the ultimate infectious entity penetrating the nuclei, the endosomal escape of MVM is very inefficient and represents the major cellular barrier for the virus to initiate the productive infection.

Concluding remarks. In the present study, we describe novel aspects in the route of MVM infection. Our results demonstrate that the early endosomal transit of MVM leads to substantial structural rearrangements of the capsid without loss of particle integrity. The extensive accumulation of MVM particles in lysosomes indicates that, although the endosomal trafficking is required for the infection, the release from this route of infectious nucleoprotein complexes able to target the nuclei is highly inefficient. The massive viral failure during the entry process would explain the high particle-to-PFU ratio typically found in parvovirus and MVM preparations. Our results also show that the endosomal pathway is a site of MVM uncoating. Further studies will elucidate whether the observed virus uncoating in the endosomal compartment is part of the infectious and/or degradative route.

ACKNOWLEDGMENTS

We thank P. Tattersall for kindly providing the antibody against N-VP1.

The work in the J.M.A. laboratory was supported by grant GR/SAL/0197/2004 from the Comunidad de Madrid and by an institutional grant from Fundación Ramón Areces to the Centro de Biología Molecular "Severo Ochoa."

REFERENCES

1. **Bantel-Schaal, U., B. Hub, and J. Kartenbeck.** 2002. Endocytosis of adeno-associated virus type 5 leads to accumulation of virus particles in the Golgi compartment. J. Virol. **76:**2340–2349.
2. **Bartlett, J. S., R. Wilcher, and R. J. Samulski.** 2000. Infectious entry pathway of adeno-associated virus and adeno-associated virus vectors. J. Virol. **74:**2777–2785.
3. **Basak, S., and H. Turner.** 1992. Infectious entry pathway for canine parvovirus. Virology **186:**368–376.
4. **Bleker, S., F. Sonntag, and J. A. Kleinschmidt.** 2005. Mutational analysis of narrow pores at the fivefold symmetry axes of adeno-associated virus type 2 capsids reveals a dual role in genome packaging and activation of phospholipase A2 activity. J. Virol. **79:**2528–2540.
5. **Canaan, S., Z. Zadori, F. Ghomashchi, J. Bollinger, M. Sadilek, M. E. Moreau, P. Tijssen, and M. H. Gelb.** 2004. Interfacial enzymology of parvovirus phospholipases A2. J. Biol. Chem. **279:**14502–14508.
6. **Clinton, G. M., and M. Hayashi.** 1976. The parvovirus MVM: a comparison of heavy and light particle infectivity and their density conversion in vitro. Virology **74:**57–63.
7. **Cotmore, S. F., A. M. D'abramo, Jr., C. M. Ticknor, and P. Tattersall.** 1999. Controlled conformational transitions in the MVM virion expose the VP1 N-terminus and viral genome without particle disassembly. Virology **254:**169–181.
8. **Cotmore, S. F., and P. Tattersall.** 1987. The autonomously replicating parvoviruses of vertebrates. Adv. Virus Res. **33:**91–174.
9. **de Duve, C.** 1983. Lysosomes revisited. Eur. J. Biochem. **137:**391–397.
10. **Ding, W., L. Zhang, Z. Yan, and J. F. Engelhardt.** 2005. Intracellular trafficking of adeno-associated viral vectors. Gene Ther. **12:**873–880.
11. **Dorsch, S., G. Liebisch, B. Kaufmann, P. von Landenberg, J. H. Hoffmann, W. Drobnik, and S. Modrow.** 2002. The VP1 unique region of parvovirus B19 and its constituent phospholipase A2-like activity. J. Virol. **76:**2014–2018.
12. **Douar, A. M., K. Poulard, D. Stockholm, and O. Danos.** 2001. Intracellular trafficking of adeno-associated virus vectors: routing to the late endosomal compartment and proteasome degradation. J. Virol. **75:**1824–1833.
13. **Dunn, W. A., Jr.** 1994. Autophagy and related mechanisms of lysosome-mediated protein degradation. Trends Cell Biol. **4:**139–143.
14. **Evans, C. J., and R. J. Aguilera.** 2003. DNase II: genes, enzymes and function. Gene **322:**1–15.
15. **Girod, A., C. E. Wobus, Z. Zadori, M. Ried, K. Leike, P. Tijssen, J. A. Kleinschmidt, and M. Hallek.** 2002. The VP1 capsid protein of adeno-associated virus type 2 is carrying a phospholipase A2 domain required for virus infectivity. J. Gen. Virol. **83:**973–978.
16. **Hansen, J., K. Qing, and A. Srivastava.** 2001. Adeno-associated virus type 2-mediated gene transfer: altered endocytic processing enhances transduction efficiency in murine fibroblasts. J. Virol. **75:**4080–4090.
17. **Hauck, B., W. Zhao, K. High, and W. Xiao.** 2004. Intracellular viral processing, not single-stranded DNA accumulation, is crucial for recombinant adeno-associated virus transduction. J. Virol. **78:**13678–13686.
18. **Hernando, E., A. L. Llamas-Saiz, C. Foces-Foces, R. McKenna, I. Portman, M. Agbandje-McKenna, and J. M. Almendral.** 2000. Biochemical and physical characterization of parvovirus minute virus of mice virus-like particles. Virology **267:**299–309.
19. **Hogle, J. M.** 2002. Poliovirus cell entry: common structural themes in viral cell entry pathways. Annu. Rev. Microbiol. **56:**677–702.
20. Reference deleted.
21. **Kronenberg, S., B. Bottcher, C. W. von der Lieth, S. Bleker, and J. A. Kleinschmidt.** 2005. A conformational change in the adeno-associated virus type 2 capsid leads to the exposure of hidden VP1 N termini. J. Virol. **79:**5296–5303.
22. **Lombardo, E., J. C. Ramírez, J. García, and J. M. Almendral.** 2002. Complementary roles of multiple nuclear targeting signals in the capsid proteins of the parvovirus minute virus of mice during assembly and onset of infection. J. Virol. **76:**7049–7059.
23. **Lombardo, E., J. C. Ramírez, M. Agbandje-Mckenna, and J. M. Almendral.** 2000. A β-stranded motif drives capsid protein oligomers of the parvovirus minute virus of mice into the nuclei for viral assembly. J. Virol. **74:**3804–3814.

24. **Lopez-Bueno, A., M. G. Mateu, and J. M. Almendral.** 2003. High mutant frequency in populations of a DNA virus allows evasion from antibody therapy in an immunodeficient host. J. Virol. **77:**2701–2708.
25. **Lux, K., N. Goerlitz, S. Schlemminger, L. Perabo, D. Goldnau, J. Endell, K. Leike, D. M. Kofler, S. Finke, M. Hallek, and H. Buning.** 2005. Green fluorescent protein-tagged adeno-associated virus particles allow the study of cytosolic and nuclear trafficking. J. Virol. **79:**11776–11787.
26. **Lyon, C. J., and R. J. Aguilera.** 1997. Purification and characterization of the immunoglobulin switch sequence-specific endonuclease (Endo-SR) from bovine spleen. Mol. Immunol. **34:**209–219.
27. **Maroto, B., J. C. Ramírez, and J. M. Almendral.** 2000. Phosphorylation status of the parvovirus minute virus of mice particle: mapping and biological relevance of the major phosphorylation sites. J. Virol. **74:**10892–10902.
28. **Maroto, B., N. Valle, R. Saffrich, and J. M. Almendral.** 2004. Nuclear export of the nonenveloped parvovirus virion is directed by an unordered protein signal exposed on the capsid surface. J. Virol. **78:**10685–10694.
29. **Mortimore, G. E.** 1987. Mechanism and regulation of induced and basal protein degradation in liver, p. 415–444. *In* H. Glaumann and F. J. Ballard (ed.), Lysosomes: their role in protein breakdown. Academic Press, New York, N.Y.
30. **Mothes, W., A. L. Boerger, S. Narayan, J. M. Cunningham, and J. A. T. Young.** 2000. Retroviral entry mediated by receptor priming and low pH triggering of an envelope glycoprotein. Cell **103:**679–689.
31. **Nurani, G., B. Lindqvist, and J. M. Casasnovas.** 2003. Receptor priming of major group human rhinoviruses for uncoating and entry at mild low-pH environments. J. Virol. **77:**11985–11991.
32. **Pajusola, K., M. Gruchala, H. Joch, T. F. Luscher, S. Yla-Herttuala, and H. Bueler.** 2002. Cell-type-specific characteristics modulate the transduction efficiency of adeno-associated virus type 2 and restrain infection of endothelial cells. J. Virol. **76:**11530–11540.
33. **Parker, J. S., and C. R. Parrish.** 2000. Cellular uptake and infection by canine parvovirus involves rapid dynamin-regulated clathrin-mediated endocytosis, followed by slower intracellular trafficking. J. Virol. **74:**1919–1930.
34. **Poranen, M. M., R. Daugelavicius, and D. H. Bamford.** 2002. Common principles in viral entry. Annu. Rev. Microbiol. **56:**521–538.
35. **Ros, C., and C. Kempf.** 2004. The ubiquitin-proteasome machinery is essential for nuclear translocation of incoming minute virus of mice. Virology **324:**350–360.
36. **Ros, C., C. J. Burckhardt, and C. Kempf.** 2002. Cytoplasmic trafficking of minute virus of mice: low-pH requirement, routing to late endosomes, and proteasome interaction. J. Virol. **76:**12634–12645.
37. **Ros, C., C. Baltzer, B. Mani, and C. Kempf.** Parvovirus uncoating *in vitro* reveals a mechanism of DNA release without capsid disassembly and striking differences in encapsidated DNA stability. Virology, in press.
38. **Rosenfeld, S. J., K. Yoshimoto, S. Kajigaya, S. Anderson, N. S. Young, A. Field, P. Warrener, G. Bansal, and M. S. Collett.** 1992. Unique region of the minor capsid protein of human parvovirus B19 is exposed on the virion surface. J. Clin. Investig. **89:**2023–2029.
39. **Rossmann, M. G., Y. He, and R. J. Kuhn.** 2002. Picornavirus-receptor interactions. Trends Microbiol. **10:**324–331.
40. **Rubio, M. P., A. Lopez-Bueno, and J. M. Almendral.** 2005. Virulent variants emerging in mice infected with the apathogenic prototype strain of the parvovirus minute virus of mice exhibit a capsid with low avidity for a primary receptor. J. Virol. **79:**11280–11290.
41. **Sanlioglu, S., P. K. Benson, J. Yang, E. M. Atkinson, T. Reynolds, and J. F. Engelhardt.** 2000. Endocytosis and nuclear trafficking of adeno-associated virus type 2 are controlled by Rac1 and phosphatidylinositol-3 kinase activation. J. Virol. **74:**9184–9196.
42. **Seisenberger, G., M. U. Ried, T. Endress, H. Buning, M. Hallek, and C. Brauchle.** 2001. Real-time single-molecule imaging of the infection pathway of an adeno-associated virus. Science **294:**1929–1932.
43. **Slor, H., H. Bustan, and T. Lev.** 1973. Deoxyribonuclease II activity in relation to cell cycle in synchronized HeLa S3 cells. Biochem. Biophys. Res. Commun. **52:**556–561.
44. **Smith, A. E., and A. Helenius.** 2004. How viruses enter animal cells. Science **304:**237–242.
45. **Suikkanen, S., K. Saajarvi, J. Hirsimaki, O. Valilehto, H. Reunanen, M. Vihinen-Ranta, and M. Vuento.** 2002. Role of recycling endosomes and lysosomes in dynein-dependent entry of canine parvovirus. J. Virol. **76:**4401–4411.
46. **Suikkanen, S., M. Antila, A. Jaatinen, M. Vihinen-Ranta, and M. Vuento.** 2003. Release of canine parvovirus from endocytic vesicles. Virology **316:** 267–280.
47. **Tattersall, P., A. J. Shatkin, and D. C. Ward.** 1977. Sequence homology between the structural polypeptides of minute virus of mice. J. Mol. Biol. **111:**375–394.
48. **Tullis, G. E., L. R. Burger, and D. J. Pintel.** 1992. The trypsin-sensitive RVER domain in the capsid proteins of minute virus of mice is required for efficient cell binding and viral infection but not for proteolytic processing in vivo. Virology **191:**846–857.
49. **Vihinen-Ranta, M., A. Kalela, P. Mäkinen, L. Kakkola, V. Marjomäki, and M. Vuento.** 1998. Intracellular route of canine parvovirus entry. J. Virol. **72:**802–806.
50. **Vihinen-Ranta, M., D. Wang, W. S. Weichert, and C. R. Parrish.** 2002. The VP1 N-terminal sequence of canine parvovirus affects nuclear transport of capsids and efficient cell infection. J. Virol. **76:**1884–1891.
51. **Vihinen-Ranta, M., L. Kakkola, A. Kalela, P. Vilja, and M. Vuento.** 1997. Characterization of a nuclear localization signal of canine parvovirus capsid proteins. Eur. J. Biochem. **250:**389–394.
52. **Vihinen-Ranta, M., W. Yuan, and C. R. Parrish.** 2000. Cytoplasmic trafficking of the canine parvovirus capsid and its role in infection and nuclear transport. J. Virol. **74:**4853–4859.
53. **Weichert, W. S., J. S. Parker, A. T. Wahid, S. F. Chang, E. Meier, and C. R. Parrish.** 1998. Assaying for structural variation in the parvovirus capsid and its role in infection. Virology **250:**106–117.
54. **Xiao, W., K. H. Warrington, Jr., P. Hearing, J. Hughes, and N. Muzyczka.** 2002. Adenovirus-facilitated nuclear translocation of adeno-associated virus type 2. J. Virol. **76:**11505–11517.
55. **Yamamoto, M.** 1971. Purification and some properties of an acid deoxyribonuclease from testes of chinook salmon Oncorhynchus tshawytscha. Biochim. Biophys. Acta **228:**95–104.
56. **Zadori, Z., J. Szelei, M. C. Lacoste, Y. Li, S. Gariepy, P. Raymond, M. Allaire, I. R. Nabi, and P. Tijssen.** 2001. A viral phospholipase A2 is required for parvovirus infectivity. Dev. Cell **1:**291–302.